JOURNAL OF OPTOELECTRONICS AND ADVANCED MATERIALS Vol. 9, No. 10, October 2007, p. 3064 - 3071

Influence of silver concentration in $Ag_x(Sb_{0.40}S_{0.60})_{100-x}$ thin amorphous films on photoinduced crystallization

J. GUTWIRTH*, T. WÁGNER, P. BEZDIČKA[a], E. KOTULÁNOVÁ[a], MIL. VLČEK[b], S. O. KASAP[c], M. FRUMAR
University of Pardubice, Faculty of Chemical Technology, Research Centre LC 523 and Department of General and Inorganic Chemistry, Legions' sq. 565, 53210 Pardubice, Czech Republic
[a] *Institute of Inorganic Chemistry, AS CR v.v.i., 25068 Husinec-Rez, Czech Republic*
[b] *Joint Laboratory of Solid State Chemistry of University of Pardubice and Institute of Macromolecular Chemistry AS CR v.v.i., Studentska 84, 53210 Pardubice, Czech Republic*
[c] *University of Saskatchewan, Department of Electrical Engineering, Campus Dr. 57, Saskatoon S7N 5A9, Canada*

Thin amorphous films from ternary system (Ag)-Sb-S were prepared as potential candidates for new phase-change memory films. Amorphous $Ag_x(Sb_{40}S_{60})_{100-x}$ thin films were deposited by thermal evaporation of $Sb_{33}S_{67}$ bulk combined with optically induced diffusion and dissolution of Ag. Prepared samples were characterized by electron microprobe (SEM-EDX), UV-Vis-NIR and Raman spectroscopy and by differential scanning calorimetry (DSC). The phase-change recording process in prepared films was tested via photocrystallization experiments done by Ar^+ ion laser. Morphology of the laser exposed dots was observed by scanning electron microscopy (SEM) and transmission optical microscopy. Micro X-ray diffraction (μ-XRD) was used for exposed dots crystallinity study. Kinetics of the phase transition was traced by measurement of optical transmission in dependence on laser exposure time (photocrystallization kinetic curve). The aim of this work is to study thermal and optical properties of prepared thin films as well as their crystallization behavior. Obtained results are discussed and confronted with the results found on thin films of the same system with different compositions and/or prepared by different techniques.

(Received July 3, 2007; accepted October 1, 2007)

Keywords: Ag-Sb-S films, Amorphous, Photoinduced crystallization

1. Introduction

Non volatile rewritable data storage is one of the recent applications of chalcogenide thin films [1 - 4]. Generally, there are two phenomena utilized for non volatile rewritable data storage based on chalcogenide thin films. First one is reversible phase change between amorphous and crystalline state and vice versa used in commercially available rewritable optical discs (such as well known CD, DVD, HD DVD or Blu-ray Discs) [5, 6] or electrically switched chalcogenide phase change memories (denoted as Ovonic Unified Memory (OUM) or Phase Change Random Acces Memory/Chalcogenide Random Acces Memory (PC-RAM, P-RAM, C-RAM)) [2, 7, 8]. Second phenomenon is electrically induced reversible dissolution and separation of metallic Ag and vice versa in system of Ag doped chalcogenide glass, denoted as Programmable Metallization Cell (PMC) Memory [9, 10, 11].

Principally, phase change is caused by laser or electrical pulses with different power and duration. Detection consists in reflectivity difference (optical memories) or electrical resistance difference (PC-RAM) of amorphous and crystalline state in case of phase change memories. Whereas, Ag dissolution in chalcogenide matrix or Ag separation from silver doped chalcogenide glass takes place via migration of Ag^+ ions caused by DC electrical pulses in programmable metallization cells. Detection is based on different electrical resistance of undoped and Ag doped chalcogenide glass.

There are some elementary considerations for material feasibility for phase change recording. These basic considerations [5] are namely on thermal and optical or electrical properties due to photo-thermal or electro-thermal origin of phase transformation as well as optical or electrical based detection, respectively. Also some properties given by practical application will be denoted.

Sufficient reflectivity contrast between amorphous and crystalline phase for detection wavelength is necessary for high Signal to Noise Ratio (SNR) which allows high speed or multilevel data storage [5, 12]. Also, sufficient absorption of both phases for writing/erasing wavelength is necessary for data recording realization. Requirements for thermal properties of recording materials are given by disc stability and stability against self crystallization during storage or during writing/erasing of neighbour data domains, respectively. Due to the first requirement, tendency to minimalize melting point T_m (typically ~ 600 °C) occurs. On the other hand, due to the second requirement, the glass transition temperature T_g must be over 100 °C. Good stability of amorphous and crystalline phase against separation during recording processes or storage is also required for achieving good cyclability (high reversibility of phase transformation) of material as well as high crystallization rate [5].

Widely used active recording films materials are based on doped Sb-Te alloys [2, 6, 12, 13]. Mostly used materials are from Ge-Sb-Te (GST) [14, 15] and Ag-In-Sb-Te (AIST) [16, 17] system, respectively.

Density Functional Theory (DFT) calculations carried out on chalcogenide materials of $AgSbCh_2$ compound [18], where Ch is S, Se or Te, suggest them to be promising materials for application as the active recording films.

Hence, there is sufficient research effort concerned about improvement current materials and research and development of new ones. Commercially used materials as GST or AIST are studied intensively due to elucidation of phase change principle at nanoscale [4, 18 - 25] or materials improving [26 - 28], while new materials e.g. from system Ag-Sb-Ch [18] where Ch is S [29 - 31] or Se [32 - 35] or Te [36 - 38]) are studied mainly in terms of thermal, optical and electrical properties and their engineering towards data storage application.

2. Experimental

Starting $Sb_{33}S_{67}$ bulk was synthesized in an evacuated quartz ampoule from elements of 5N purity in electric rocking furnace. Preliminary pressure in the ampoule was ~ 10^{-3} Pa, synthesis temperature was T ~ 750 °C during time t = 24 hours. Polycrystalline bulk was obtained by cooling of the ampoule with the melt in water (T ~ 10 °C). Composition and homogeneity of prepared bulk was checked by SEM-EDX technique proved on apparatus Jeol JSM – 5500 LV equipped with analyser IXRF Systems and Gresham Sirius 10 detector. Accelerating voltage was U = 20 kV.

Prepared bulk was used as a source for thermal evaporation (TE) of Sb-S thin films. Thin films were prepared in thermal evaporator Tesla UP 858 from silica glass crucible heated by molybdenum spiral. Background pressure was p ~ 10^{-4} Pa and the deposition rate ~ 2 nm*s^{-1}. Deposition rate and thickness were controlled by quartz crystal monitor. The homogeneity of prepared thin films was guaranteed by planetary rotation of substrates (microscope slides). Thickness of prepared thin films was ~ 720 nm.

Thin $Ag_x(Sb_{0.40}S_{0.60})_{100-x}$ films were prepared from host $Sb_{40}S_{60}$ films by optically induced diffusion and dissolution (OIDD) [39, 40] of Ag. Silver was step-by-step added in two steps as thermally evaporated thin (d ~ 5 nm) films on top of $Sb_{40}S_{60}$ host matrix. TE of Ag was carried out directly from molybdenum boat in the same system, at preliminary pressure p ~ 10^{-4} Pa and deposition rate ~ 0.3 nm*s^{-1}. The bilayer system ($Sb_{40}S_{60}$/Ag in first step or $Ag_{1.1}(Sb_{0.4}S_{0.6})_{98.9}$/Ag in second step) was illuminated from chalcogenide glass side by a tungsten lamp focused by large Fresnel lens with IR cut-off filter (I ~ 80 mW*cm^{-2}) which results in homogeneous amorphous $Ag_x(Sb_{0.40}S_{0.60})_{100-x}$ thin films.

The composition, composition homogeneity and surface quality of prepared films were checked by SEM-EDX technique proved on the same apparatus and under the same conditions as written above. Back-scattered electron (BSE) signal in low vacuum mode was used for projection.

The structure of prepared bulk and thin films was studied by Raman spectroscopy on FT Raman spectrometer Bruker IFS/FRA 55 equipped with Nd-YAG laser (λ = 1064 nm) and N_2 (l) cooled Ge detector. There were realized 100 scans with laser output P = 50 mW and resolution 4 cm^{-1}.

Thermal properties of prepared thin films were studied by differential scanning calorimetry (DSC). DSC measurements were carried out via TA Instruments DSC-2910 apparatus when temperature gradient 5 °C*min^{-1} was applied.

Optical transmission spectra were recorded on UV-Vis-NIR dispersive spectrophotometer Jasco V-570. The resolution was 2 nm and scan speed 400 nm*s^{-1}. Spectral data were evaluated by Swanepoel method [41] to acquire the film thickness d and refractive index n. Optical band gap energy (E_g^{opt}) was evaluated from intercept on the energy axis of linear fit of high absorbing region ($\alpha \geq 10^4$ cm^{-1}) in plot $(\alpha h\omega)^{1/2}$ versus $h\omega$ (where α is absorption coefficient and $h\omega$ is energy of incident photons) known as Tauc extrapolation [42]. Software WinSwan ver. 1.01 developed at University of Pardubice was used for both these evaluations.

Possibility of application as an active material for rewritable optical data storage was tested via dot laser exposures. Dot laser exposures were carried out by Ar^+ ion laser Coherent Innova 300C (λ = 514.5 nm) of output power P = 845.5 mW and beam diameter d = 1.1 mm (i.e. intensity I = 89 W*cm^{-2}). Exposition time was scaled from 1 s to 20 s.

Dot laser exposures were characterized by several techniques, i.e. by transmission optical microscopy, scanning electron microscopy (SEM), micro X-ray diffraction (μ-XRD) and by measurement of photocrystallization kinetic curves (i.e. measurement of optical transmission in dependence on laser exposure time).

Transmission optical microscopy was realized via standard microscope Carl Zeiss Jena equipped with digital camera Nikon Coolpix 990. SEM-EDX study was carried out on the same apparatus and under the identical conditions as in case of thin films.

Micro-XRD was measured by diffractometer PANalytical X'PertPRO with Co Kα X-ray tube (U = 30 kV, I = 45 mA) and Fe β filter. Primary optics

was silica monocapillary (diameter d = 0.1 mm), secondary optics was Soller slits (0.04 rad). Multichannel semiconductor detector PANalytical X'celerator with anti-scatter shield was used for detection. Qualitative analysis was performed with HighScore software package (PANalytical, The Netherlands, version 1.0d), Diffrac-Plus software package (Bruker AXS, Germany, version 8.0) and JCPDS PDF-2 database [43].

Photorystallization kinetic curves (dependence of optical transmission on laser exposure time) were collected by Schnellphotometer Carl Zeiss Jena with photomultiplier and optical system Opton. Polychromatic light with circular beam of diameter d = 120 μm was used for measurement.

3. Results

Composition (SEM-EDX) of prepared thin $Ag_x(Sb_{0.40}S_{0.60})_{100-x}$ films is listed together with film thickness d obtained by Swanepoel method [41] and optical band gap energy E_g^{opt} determined by Tauc extrapolation [42] in Table 1. Maximum obtained silver concentration in thin films is 3.5 at. % .

Table 1. Composition (SEM-EDX), thickness d and optical band gap energy E_g^{opt} of prepared thin films.

Sample	Composition [at %]	d [nm]	E_g^{opt} [eV]
b2-0	$Sb_{40}S_{60}$	722	1.67
b2-5	$Ag_{1.1}(Sb_{40}S_{60})_{98.9}$	730	1.61
b2-10	$Ag_{2.4}(Sb_{40}S_{60})_{97.6}$	744	1.58

]Structure of prepared bulk and thin films was proved by Raman spectroscopy, spectra are presented in Fig. 1. Raman bands maxima which belong to amorphous phase (thin films) are marked above spectra, vibration frequencies which belong to crystalline phase (bulk) are summarized under spectra, respectively. Raman spectra were interpreted following [44, 45]: broad band with maximum at 292 cm^{-1} (thin films) and bands with maxima at 282 cm^{-1} and 311 cm^{-1} (bulk) are assigned [44, 45] to vibrations of $SbS_{3/2}$ units. Band with maximum at 170 cm^{-1} is assigned to Sb-Sb vibrations in S_2Sb-SbS_2 units and bands with maxima at 140 cm^{-1} and 475 cm^{-1} to vibration of S-rings fragments [44]. Bands with maxima at 241 cm^{-1}, 195 cm^{-1}, 155 cm^{-1}, 128 cm^{-1} could be assigned to vibrations of crystalline Sb_2S_3 [45].

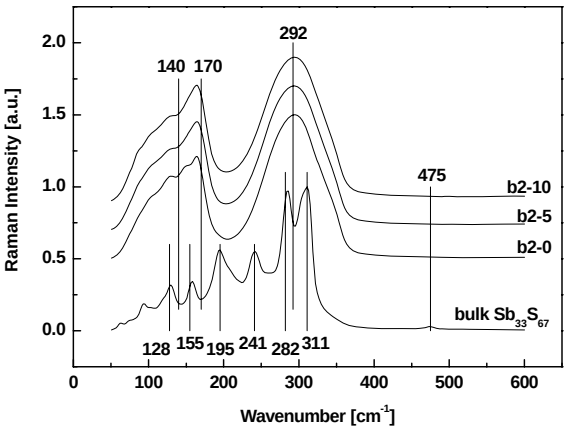

Fig. 1. Raman spectra of prepared bulk and thin films. Vibration frequencies which belong to amorphous phase are summarized above spectra, vibration frequencies which belong to crystalline phase are summarized under spectra, respectively.

DSC curves of prepared thin films were measured, characteristic temperatures (glass transition temperature T_g, crystallization temperature T_c and melting temperature T_m) are summarized in Table 2. DSC curves (depicted at Fig. 2) are evaluated on basis of known chemical composition of prepared samples (Table 1), identification of photocrystallized products established by μ-XRD (see below Fig. 6) and phase diagrams [46, 47]. Our previous results [30, 31, 48] were taken into account as well.

Table 2. Thermal properties (glass transition temperature T_g, crystallization temperature T_c and melting temperature T_m) of prepared thin films obtained by DSC technique. NA denotes, that value has not been obtained, dash denotes, that particular product is not present in the sample.

Sample	T_g [°C]	T_c Sb_2S_3 [°C]		T_c Ag_3SbS_3 [°C]		T_m Sb_2S_3 [°C]		T_m Ag_3SbS_3 [°C]	
		onset	peak	onset	peak	onset	peak	onset	peak
b2-0	221	257.8	265.4	-	-	NA	NA	-	-
b2-5	175	234.7	239.8	219.7	227.3	445.8	448.0	NA	NA
b2-10	180	230.5	236.5	218.6	223.4	440.3	442.9	373.6	375.7

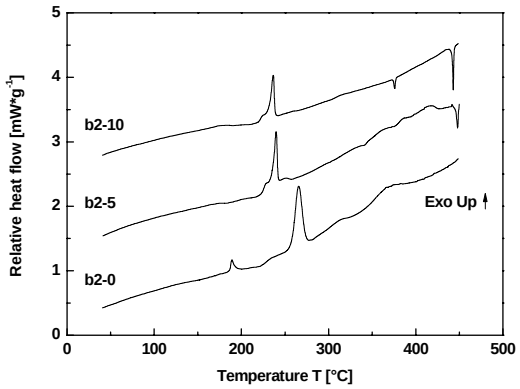

Fig. 2. DSC curves of prepared thin films.

Optical transmission spectra of prepared samples are plotted in Fig. 3. Spectral dependence of refractive index n (obtained by spectra evaluation as described by Swanepoel [41]) fitted by Cauchy dispersion function is presented in Fig. 4.

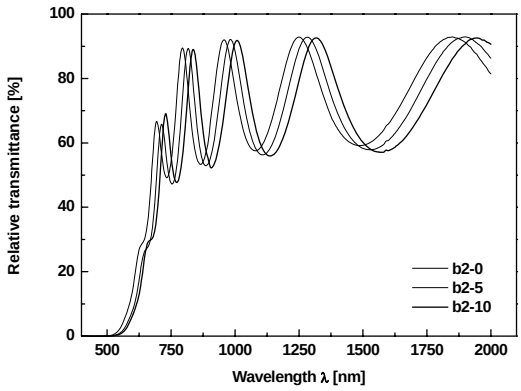

Fig. 3. UV-Vis-NIR spectra of prepared thin films.

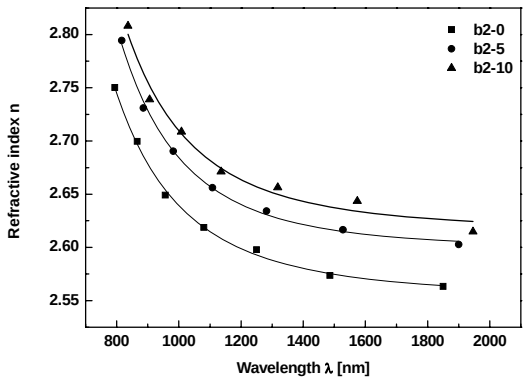

Fig. 4. Spectral dependence of refractive index of prepared thin films. Experimentally obtained points are fitted by Cauchy dispersion function.

Transmission optical microscopy and SEM photographs of Ar^+ ion laser exposed dots with exposure time $t_{EXP} = 20$ s are plotted in Fig. 5 for all prepared samples. Left upper insert in SEM photographs is unexposed film for comparison; scale is the same. Diffraction patterns of unexposed film and laser exposed dot (exposure time $t_{EXP} = 20$ s) for all samples are presented in Fig. 6. Photocrystallization kinetic curves are plotted in Fig. 7.

4. Discussion

From EDX analysis (Table 1) could be concluded, that melt-quench process produces macroscopically homogeneous $Sb_{33}S_{67}$ bulks. Character (amorphous/crystalline) studied by Raman spectroscopy depends on quenching conditions and it is in interval from amorphous (intensive quenching of small batches in water/ice mixture) to polycrystalline (quenching on air or in water). Sometimes phase separation of sulfur can occur during quenching.

Thin films with composition $Sb_{40}S_{60}$ (i.e. stoichiometric Sb_2S_3) can be thermally evaporated from bulk of $Sb_{33}S_{67}$ composition if evaporation rate is low [29, 48]. Thickness of amorphous film increase monotonously during silver doping (as seen in Table 1) in contrast to films prepared by OIDD of Ag into thin $Sb_{33}S_{67}$ films (further marked as $Ag_x(Sb_{33}S_{67})_{100-x}$ samples) where significant thickness decrease occurs after first silver introduction [29, 31, 48].

Structure of bulk and prepared films was studied by Raman spectroscopy; spectra (presented in Fig. 1) are evaluated on basis of [44, 45]. From desintegration and sharpening of the broad band with maximum at 292 cm^{-1} to the bands with maxima at 282 cm^{-1} and 311 cm^{-1} is deduced, that while films are amorphous, bulk contains crystalline portion. S-ring fragments vibration band (with maximum at 475 cm^{-1}) which disappears in b2-0 sample spectrum in comparison to bulk spectrum clearly indicates sulfur depletion during evaporation. With increasing silver content is visible increasing intensity of band with maximum 170 cm^{-1} (Sb-Sb bonds vibrations). From this, preferential bonding between silver and sulfur atoms can be deduced. This is also supported by fact, that larger amount of Ag was photodissolved in system $Sb_{33}S_{67}$ [29, 31, 48].

Thermal properties (T_g, T_c and T_m) studied by DSC are presented in Table 2. It is clear, that with increasing silver concentration decrease all characteristic temperatures except $T_m(Ag_3SbS_3)$ where data are insufficient and T_g, where significant decreasing of T_g after first silver doping followed by T_g increasing in next step occur. Observed characteristic temperatures are higher, than in case of $Ag_x(Sb_{33}S_{67})_{100-x}$ samples [29, 31].

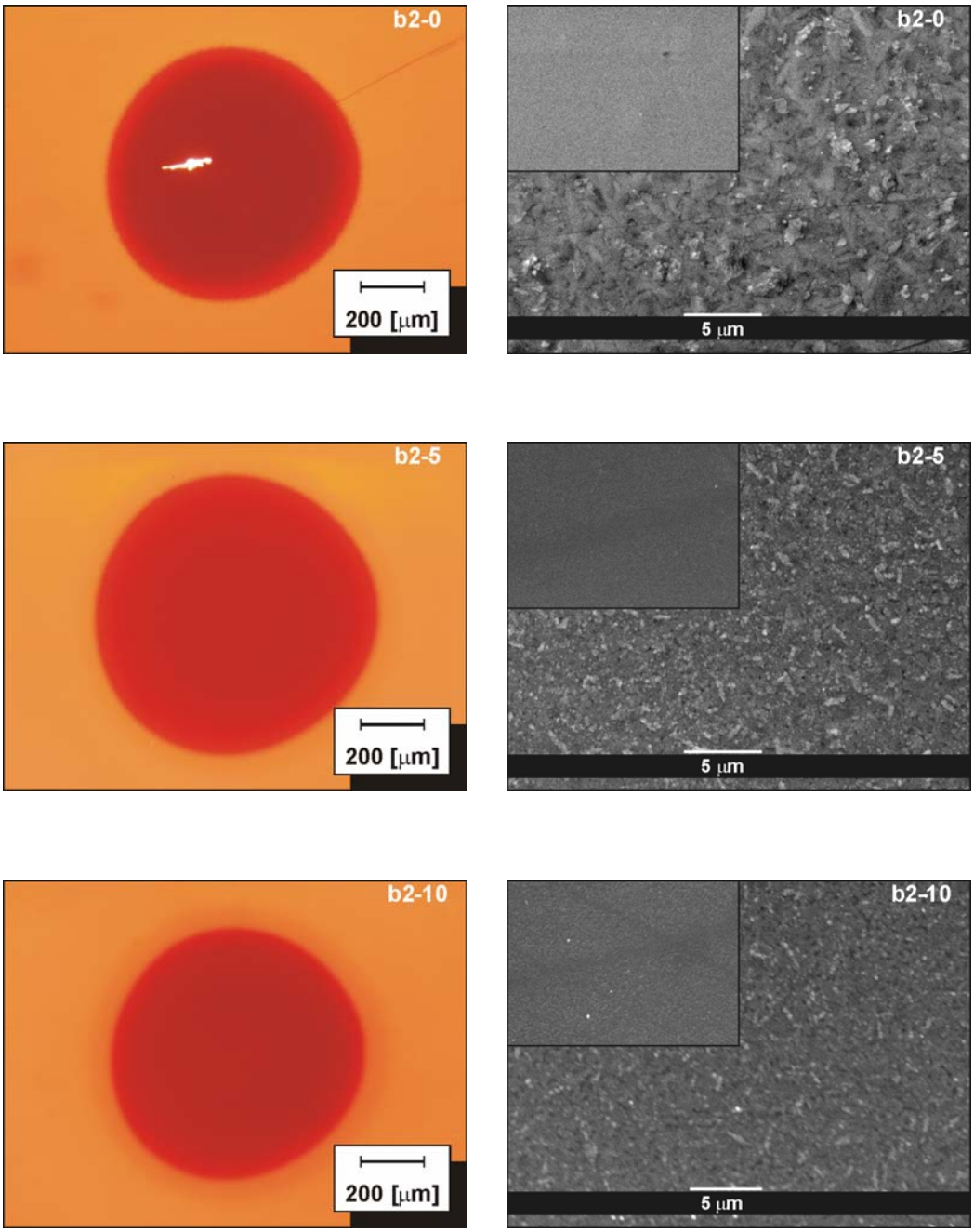

Fig. 5. Transmission optical microscopy and SEM photographs of laser exposed dots (exposure time t_{EXP} = 20 s) for all prepared samples. Insert in SEM photographs is unexposed film for comparison.

Red shift (decrease of E_g^{opt}) with increasing silver content was observed. This fact is visible from spectral dependence of transmission (Fig. 3) and E_g^{opt} values listed in Table 1. Refractive index n increases with increasing silver content as visible in Fig. 4. Good quality and homogeneity of prepared (Ag)-Sb-S thin films were confirmed by optical transmission spectra where no shrinkage of interference fringes was observed [49].

Photoinduced crystallization of prepared thin films was tested by Ar^+ ion laser exposures. Transmission optical microscopy and SEM photographs of exposed dot (t_{EXP} = 20 s) of all prepared samples are shown in Fig. 5. Insert in left upper corner of SEM images is SEM

photography of unexposed thin film. These photographs together with micro-XRD patterns presented in Figure 6. clearly show amorphous origin of unexposed thin films and crystalline origin of exposed dots. There were no hallo effect observed, except narrow ring, in contrast to $Ag_x(Sb_{33}S_{67})_{100-x}$ samples [30, 31]. Origin of the narrow hallo ring observed by transmission optical microscopy could be seen due to thermal distribution which is influenced by Gaussian laser beam profile and thermal conductivity of thin film. No compositional deviation in this hallo ring was observed. μ-XRD was used not only for determination of crystallinity of dot laser exposures, but also for identification of crystalline phases. All samples contain orthorhombic Sb_2S_3 as main crystalline phase; Ag doped samples contain also rhombohedral Ag_3SbS_3 as a minor crystalline phase.

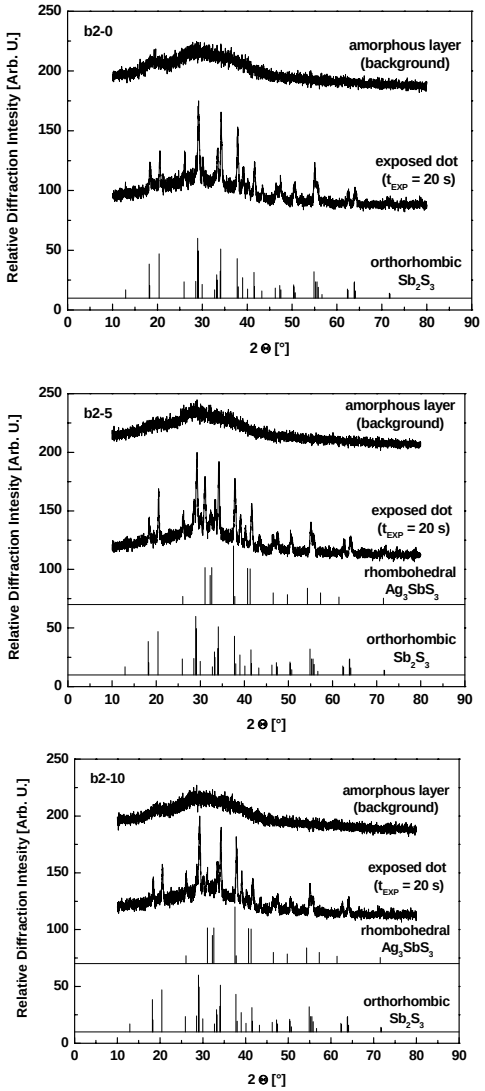

Fig. 6. μ-XRD pattern of laser exposed dot (exposure time t_{EXP} = 20 s) and unexposed film for all prepared samples.

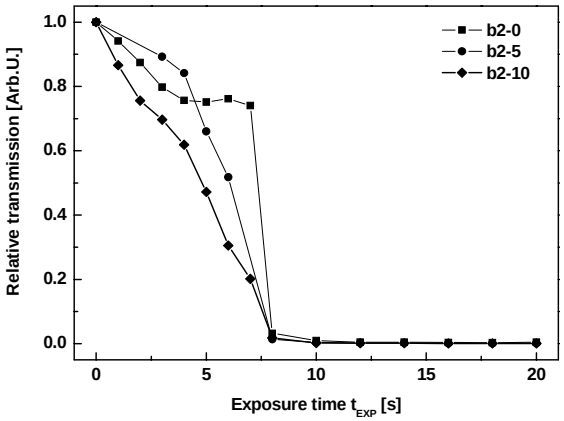

Fig. 7. Photocrystallization kinetic curves (dependence of optical transmission on Ar^+ ion laser exposure time) of prepared samples. Lines are added for eye-guiding.

The fact, that Ag influences only induction period of crystallization, while the total time of crystallization (i.e. ~ 8 s) doesn't change, could be seen in photocrystallization kinetic curves (Fig. 7). This result is in contrast to results obtained on $Ag_x(Sb_{33}S_{67})_{100-x}$ samples, where silver influenced not only initial stage, but also strongly reduce total time of the crystallization [31]. Also, while curve profiles of $Ag_x(Sb_{33}S_{67})_{100-x}$ samples are simple sigmoidal [31], profiles presented at Fig. 7 are more complicated, so different and probably more complex mechanism of laser induced crystallization could be expected.

5. Conclusion

Thin amorphous $Ag_x(Sb_{0.40}S_{0.60})_{100-x}$ films up to silver concentration c_{Ag} = 3.5 at. % were prepared by thermal evaporation of $Sb_{33}S_{67}$ bulk and optically induced diffusion and dissolution of Ag. Amorphous character and homogeneity of prepared films were proved by several techniques (μ-XRD, SEM-EDX and UV-Vis-NIR spectrometry). Some parameters as optical band gap energy E_g^{opt}, spectral dependence of refractive index n and characteristic temperatures (glass transition temperature T_g, crystallization temperature T_c and melting temperature T_m) and their evolution with silver doping were presented and compared with samples prepared by OIDD of Ag into $Sb_{33}S_{67}$ host matrix [31].

Photocrystallization experiments were successfully carried out. Crystallization products were clarified as orthorhombic Sb_2S_3 and rhombohedral Ag_3SbS_3 in case of Ag doped samples, respectively. Crystallization kinetic was traced. Nevertheless, total time of crystallization of prepared samples, which was found to be independent on Ag concentration, is higher in comparison with $Ag_x(Sb_{33}S_{67})_{100-x}$ samples [31]. Also, $Ag_x(Sb_{33}S_{67})_{100-x}$ samples are preferred [18] due to their tendency to crystallize as cubic $AgSbS_2$ in contrast to rhobohedral Ag_3SbS_3.

Acknowledgements

The authors thank to the Ministry of Education, Youth and Sports (Research Centre LC 523 project and project MSM 0021627501), the Czech Science Foundation (project GA 203/06/1368 and project AVOZ 40500505) for financial support.

References

[1] T. D. Milster in: Th. G. Brown, K. Creath, H. Kogelnik, M. A. Kriss, J. Schmit, M. J. Weber (eds.), The Optics Encyclopedia – Basic Fundations and Practical Applications Volume 1, Wiley-VCH, Weinheim, Germany (2004), p. 227 – 274.
[2] M. Wuttig in: R. Waser (ed.), Nanoelectronics and Information Technology, Advanced Electronic Materials and Novel Devices, Wiley VCH, Weinheim, Germany (2003), p. 645 – 658.
[3] M. Wuttig, Nat. Mater. **4**(4), 265 – 266 (2005).
[4] C. Steimer, W. Welnic, J. Kalb, M. Wuttig, J. Optoelectron. Adv. Mater. **8**(6), 2044 – 2050 (2006).
[5] H. J. Borg, R. van Woudenberg, J. Magn. Magn. Mater. **193**(1-3), 519 – 525 (1999).
[6] G. F. Zhou, Mater. Sci. Eng. A – Struct. Mater. Prop. Microstruct. Process. **304** (Spec. Iss.), 73 - 80 (2001).
[7] G. Purvis, III-Vs Review **19**(8), 39 – 41 (2006).
[8] A. L. Lacaita, Solid-State Electron. **50**(1), 24 – 31 (2006).
[9] M. N. Kozicki, M. Mitkova, J. Non-Cryst. Solids **299-302** Part 2, 1023 – 1027 (2002).
[10] M. N. Kozicki, M. Mitkova, M. Park, M. Balakrishnan, C. Gopalan, Superlattices Microstruct. **34**(3-6), 459 – 465 (2003).
[11] M. N. Kozicki, M. Mitkova, J. Non-Cryst. Solids **352**(6-7), 567 - 577 (2006).
[12] T. Ohta, J. Optoelectron. Adv. Mater. **3**(3), 609 – 626 (2001).
[13] T. Ohta, K. Nishiuchi, K. Narumi, Y. Kitaoka, H. Ishibashi, N. Yamada, T. Kozaki, Jpn. J. Appl. Phys. **39** (2B Part 1), 770-774 (2000).
[14] B. Hyot, L. Poupinet, V. Gehanno, P. J. Desre, J. Magn. Magn. Mater. **249**(3), 504-508 (2002).
[15] H. Dieker, M. Wuttig, Thin Solid Films **478**(1-2), 248-251 (2005).
[16] J. Li, L.Hou, H. Ruan, Q. Xie, F. Gan, Proc. SPIE **4085**, 125 – 128 (2001).
[17] J. Li, F. Gan, Thin Solid Films **402**(1-2), 232-236 (2002).
[18] W. Welnic, A. Pamungkas, R. Detemple, C. Steimer, S. Blugel, M. Wuttig, Nat. Mater. **5**(1), 56 - 62 (2006).
[19] F. Gan, J. Non-Cryst. Solids **256-257**(2), 176 – 182 (1999).
[20] A. V. Kolobov, P. Fons, A. I. Frenkel, A. L. Ankudinov, J. Tominaga, T. Uruga, Nat. Mater. **3**(10), 703 – 708 (2004) .
[21] H. Tashiro, M. Harigaya, Y. Kageyama, K. Ito, M. Shinotsuka, K. Tani, A. Watada, N. Yiwata, Y. Nakata, S. Emura, Jpn. J. Appl. Phys. **41** (6A part 1), 3758 – 3759 (2002).
[22] J. Kalb, F. Spaepen, M. Wuttig, J. Appl. Phys. **93**(5), 2389 – 2393 (2003).
[23] A. V. Kolobov, P. Fons, J. Tominaga, T. Uruga, J. Non-Cryst. Solids **352**(9 – 20), 1612 – 1615 (2006).
[24] M. A. Paesler, D. A. Baker, G. Lucovsky, A. E. Edwards, P. C. Taylor, J. Optoelectron. Adv. Mater. **8**(6), 2039 - 2043 (2006).
[25] A. V. Kolobov, J. Haines, A. Pradel, M. Ribes, P. Fons, J. Tominaga, J. Optoelectron. Adv. Mater. **8**(6), 2161 – 2163 (2006).
[26] B. Liu, Z. Song, T. Zhang, S. Feng, B. Chen, Appl. Surf. Sci. **242**(1-2), 62 – 69 (2005).
[27] B. Liu, Z. Song, T. Zhang, J. Xia, S. Feng, B. Chen, Thin Solid Films **478**(1-2), 49 – 55 (2005).
[28] Su-Shia Lin, Ceram. Int. **In Press** (2006), doi:10.1016/j.ceramint.2006.03.020.
[29] J. Gutwirth, T. Wagner, S. O. Kasap, M. Frumar, J. Optoelectron. Adv. Mater. **7**(4), 1813 – 1821 (2005).
[30] J. Gutwirth, T. Wagner, P. Bezdicka, J. Pokorny, Mil. Vlcek, M. Frumar, J. Non-Cryst. Solids **351**(43-45), 3556 – 3561 (2005).
[31] J. Gutwirth, T. Wagner, P. Bezdicka, Mil. Vlcek, S. O. Kasap, M. Frumar, J. Non-Cryst. Solids **353**(13-15), 1431 – 436 (2007).
[32] N. Mehta, M. Zulfequar, A. Kumar, Phys. Status Solidi A – Appl. Mat. **203**(2), 236 – 246 (2006).
[33] N. Mehta, R. S. Tiwari, A. Kumar, Mat. Res. Bull. **41**(9), 1664 - 1672 (2006).
[34] Tz. Babeva, D. Dimitrov, S. Kitova, I. Konstantinov, Vacuum **58**(2-3), 496 - 501 (2000).
[35] K. Wang, C. Steimer, R. Detemple, D. Wamwangi, M. Wuttig, Appl. Phys A-Mater. Sci. Process. **81**(8), 1601 – 1605 (2005).
[36] Y. D. Sharma, R. K. Bhatnagar, Opt. Eng. **41**(7), 1668 – 1673 (2002).
[37] J. Xu, B. Liu, Z. Song, S. Feng, B. Chen, Mater. Sci. Eng. B-Solid State Mater. Adv. Technol. **127**(2-3), 228 – 232 (2006).
[38] B. Liu, Z. Song, S. Feng, B. Chen, Microelectron. Eng. **82**(2), 168 - 174 (2005).
[39] T. Wagner, A. Mackova, V. Perina, E. Rauhala, A. Seppälä, S. O. Kasap, M. Frumar, Mir. Vlcek, Mil. Vlcek, J. Non-Cryst. Solids **299-302 Part 2**, 1028 – 1032 (2002).
[40] M. Frumar, T. Wagner, Curr. Opin. Solid State Mat. Sci. **7**(2), 117-126 (2003).
[41] R. Swanepoel, J. Phys. E-Sci. Instrum. **16**, 1214 – 1222 (1983).
[42] J. Tauc, in: J. Tauc (Ed.), Amorphous and Liquid Semiconductors, Plenum, New York, USA, (1974).
[43] JCPDS PDF-2 database, International Centre for

Diffraction Data, Newtown Square, PA, U.S.A., release 54, (2004).
[44] I. Watanabe, S. Noguchi, T. Shimizu, J. Non-Cryst. Solids **58**(1), 35-40 (1983).
[45] B. Minceva-Sukarova, G. Jovanovski, P. Makreski, B. Soptrajanov, W. Giffith, R. Willis, I. Grzetic, J. Mol. Struct. **651-653**, 181 - 189 (2003).
[46] P. Villars, A. Prince, H. Okamoto in Handbook of Ternary Alloy Phase Diagrams Vol. 3, ASM International, USA, (1995).
[47] H. Okamoto P. R. Subramanian, L. Kacprzak in Handbook of Binary Alloy Phase Diagrams Second Edition Vol. 1, ASM International, USA, (1992).
[48] J. Gutwirth, T. Wagner, P. Bezdicka, M. Vlcek, M. Frumar, Phys. Chem. Glasses **47**(2), 229 - 232 (2006).
[49] T. I. Kosa, T. Wagner, P. J. S. Ewen, A. E. Owen, Philos. Mag. B **71**(3), 311 - 318 (1995).

*Corresponding author: Jan.Gutwirth@upce.cz